# DGAI: Decoupled On-Disk Graph-Based ANN Index for Efficient Updates and Queries

Jiahao Lou<sup>†</sup>, Quan Yu<sup>†</sup>, Shufeng Gong<sup>†</sup>, Song Yu<sup>†</sup>, Yanfeng Zhang<sup>†</sup>, Ge Yu<sup>†</sup>

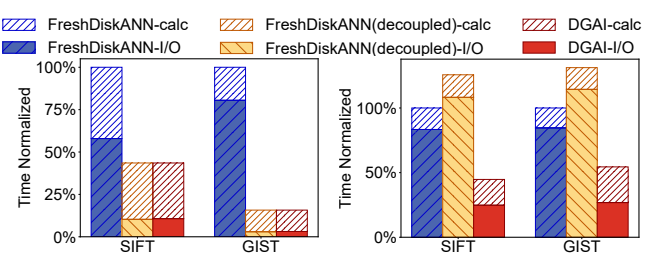
<sup>†</sup>Northeastern University, China

#### **Abstract**

On-disk graph-based indexes are widely used in approximate nearest neighbor (ANN) search systems for large-scale, high-dimensional vectors. However, traditional coupled storage methods, which store vectors within the index, are inefficient for index updates. Coupled storage incurs excessive redundant vector reads and writes when updating the graph topology, leading to significant invalid I/O. To address this issue, we propose a decoupled storage architecture. While a decoupled architecture reduces query performance. To overcome this limitation, we design two tailored strategies: (i) a three-stage query mechanism that leverages multiple POcompressed vectors to filter invalid I/O and computations, and (ii) an incremental page-level topological reordering strategy that incrementally inserts new nodes into pages containing their most similar neighbors to mitigate read amplification. Together, these techniques substantially reduce both I/O and computational overhead during ANN search. Experimental results show that the decoupled architecture improves update speed by  $10.05 \times$  for insertions and  $6.89 \times$  for deletions, while the three-stage query and incremental reordering enhance query efficiency by 2.66× compared to the traditional coupled architecture.

#### 1 Introduction

Approximate nearest neighbor search (ANNS) plays a critical role in various real-world applications, such as information retrieval [11,37,40,49], recommendation systems [17,36,38,41], and large language models (LLMs) [14, 19, 26–28, 30, 39, 42, 54]. Graph-based indices, such as HNSW [33] and Vanama [24], are widely used to enable efficient ANNS on high-dimensional vectors. In these indices, vectors are organized as a directed graph, where each node corresponds to a vector, and edges are established according to distance relationships. To support larger high-dimensional vector datasets, indices are typically stored on disk [43], as they are difficult to fit entirely into the memory of a commodity PC [47].



(a) Update time breakdown

(b) Query time breakdown

Figure 1: The update and ANNS query time (breakdown) comparison, where the update only contains deleted vectors. The -calc and -I/O mean the time spent on computing and disk I/O.

Most existing graph-based indices [18, 24, 32, 33], along with their algorithm-level [47, 57] and system-level optimizations [22, 56, 58], primarily focus on query efficiency, while overlooking the dynamic nature of vector datasets in real scenarios, which frequently evolve through the addition of new vectors and the deletion of outdated ones over time. For instance, in e-commerce platforms like Amazon [2] that support image-based product search, users can find similar products by uploading an image. The system then encodes this image into a vector and performs ANNS to retrieve similar products from the database. As products change frequently, with new items being added and sold-out items being removed, the vector set evolves over time. Subsequently, the index should be updated to maintain query efficiency and accuracy.

Recently, several dynamic ANNS systems have been proposed to support these dynamic scenarios [6,23,31,43,50,51]. However, existing graph-based dynamic ANNS systems usually exhibit poor update performance due to high I/O overhead. For example, in the representative dynamic ANNS system FreshDiskANN [43], we evaluate the update overhead on two real-world datasets (SIFT and GIST), where 0.1% of the vectors are deleted. The results are shown in Figure 1a. It can be seen that I/O accounts for 57.9–80.5% of the total update time.

<sup>\*</sup>Corresponding author: Shufeng Gong (gongsf@mail.neu.edu.cn)

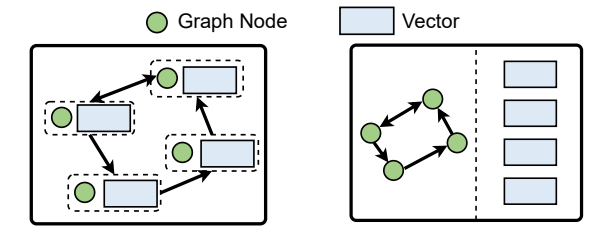
Motivation. The underlying cause is the coupled storage scheme, in which vectors are stored within the index's topology, as shown in Figure 2a. Vector updates themselves are lightweight, involving the insertion or deletion of corresponding elements within the vectors. In contrast, topological updates are considerably more complex, especially for node deletion, which requires the removal of nodes and their edges, as well as the subsequent repair of the affected nodes, i.e., incoming and outgoing neighbors of the deleted nodes. Since the vector and its corresponding node are stored together, topological updates inevitably involve simultaneous reads and writes on the associated vectors, introducing substantial redundant I/O overhead (more than 79%). Such inefficiency motivates our design of the decoupled storage architecture.

<u>Decoupled Storage Architecture</u>. An intuitive solution is to decouple the storage architecture, separating the I/O-intensive graph topology from the vector data whose updates incur lower I/O overhead, as shown in Figure 2b. This decoupled storage architecture eliminates redundant I/O on vectors and allows updates to focus solely on the graph topology, thereby improving update performance. As shown in Figure 1a, FreshDiskANN with the decoupled design reduces the total update time by 56% to 84% compared to the coupled baseline.

However, we observe that such a design leads to a notable degradation in query performance. As shown in Figure 1b, the decoupling of topology and vector data incurs an increase in query latency of more than 23%. In existing graph-based ANNS, expanding a new node requires reading the topology of the node and its associated vector to compute the exact distance to the query vector. This query strategy amplifies both the number and volume of I/O operations on the decoupled storage architecture (Section 3.2), with two read actions per query step (one for the topology and one for the vector), involving two 4KB page accesses. In contrast, the coupled storage architecture performs only a single read operation per step, involving a single 4KB page access.

**Dilemma & Challenge**. From the above analysis, the updatefriendly decoupled topology-vector storage architecture and the query-friendly coupled storage architecture exhibit fundamentally conflicting structural requirements, making it challenging to design a graph-based index that supports both efficient updates and queries simultaneously.

Opportunity. In the coupled storage architecture, page-based data access inevitably incurs redundant I/O during updates, since topology modifications also involve unnecessary I/Os on co-located vector data within the same page, making it challenging to optimize updates. In the decoupled architecture, avoiding the simultaneous retrieval of topology and vectors during query execution can substantially reduce I/O overhead, thereby offering an opportunity to improve query efficiency. We therefore turn to designing an efficient query strategy tailored to the decoupled storage architecture.



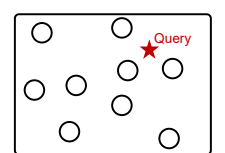
(a) Coupled topology–vector (b) Decoupled topology–vector Figure 2: Coupled vs. decoupled storage architecture.

Multi-PQs based Three-Stage Query Strategy for Decoupled Storage Architecture. To address the query inefficiencies caused by decoupling the topology from the index vectors, we propose a three-stage query strategy tailored to the decoupled architecture, which involves multiple product quantizations (PQs). Specifically, when traversing the graph topology, we only leverage a set of PQ-compressed vectors (abbr. PQ-vectors) for distance comparisons and generate ANN candidates. Then we utilize other PQs to filter candidates, producing fewer yet more accurate ones. Finally, we retrieve the vectors of candidates from disk for precise distance computations and comparisons, yielding the final results. In this way, as the number of candidates decreases after filtering, both the I/O overhead of vector retrieval and the computational cost of distance calculation are reduced.

<u>Similarity-Aware Incremental Reordering.</u> Furthermore, the decoupled design allows each page to store more topology information, enabling each disk read to retrieve more of it. To effectively utilize this additional information, we propose an incremental topology reordering method that enables the retrieved topology data to be immediately reused in subsequent operations. In combination with buffering, this approach significantly reduces the number of disk reads required for graph traversal.

In summary, we make the following contributions.

- We propose a decoupled graph-based ANNS storage architecture that separates the vectors from the graph topology based on a thorough analysis of existing ANNS systems.
   This decoupled design greatly improves the update performance of the graph-based index.
- Building on this decoupled architecture, we propose an efficient three-stage query strategy by leveraging the multiple PQs and a similarity-aware incremental topology reordering to minimize read amplification during graph traversal.
- We implement DGAI, a high-performance dynamic graphbased index for billion-scale ANNS tasks upon a decoupled storage architecture. Extensive experiments on realworld datasets demonstrate that DGAI achieves substantial improvements in both update and query efficiency compared to state-of-the-art disk-based systems, while maintaining comparable search accuracy.







(a) Vector data

(b) Graph-based index

(c) Index layout

Figure 3: An example of a graph-based vector index on a vector dataset.

#### 2 Background

In this section, we introduce some fundamental concepts and key techniques of approximate nearest neighbor search.

Approximate Nearest Neighbor Search (ANNS). Given a dataset  $\mathcal{V} = \{V_1, V_2, \dots, V_n\} \subset \mathbb{R}^D$  of n vectors in d-dimensional space and a query vector  $V_q \in \mathbb{R}^D$ , the ANNS aims to identify the k vectors  $\mathcal{V}_q^k \subset \mathcal{V}$  most close to the query  $V_q$  based on some distance rules [18, 24, 32, 33]. The query accuracy is measured by the recall value  $recall@k = (\mathcal{V}_q^k \cap \mathcal{V}_q^{\prime k})/\mathcal{V}_q^{\prime k}$ , where  $\mathcal{V}_q^{\prime k}$  is the exact top-k nearest neighbor of  $V_q$  in  $\mathcal{V}$ .

**Graph-Based Index.** Graph-based index treats each vector as a node and constructs a directed graph based on distance rules. In Figure 3b, we present an example of a graph-based index constructed for the vector dataset in Figure 3a. For each node, the outdegree is bounded by a predefined threshold *R*, thereby preventing query performance degradation due to the overhead of calculating and comparing distances with too many number of neighbors during ANNS.

In ANNS, graph-based methods utilize a best-first greedy search [12, 22, 24, 33]. As shown in Algorithm 1, best-first greedy search maintains an ANN candidate queue with a fixed size, containing the current top-l nearest vectors sorted by the distance. The search starts with a fixed entry node and gets closer to the query vector step by step. Each step will expand the current closest node and add its neighbors to a candidate queue, until all the nodes in the queue is expanded. This greedy graph traversal quickly gets approximate nearest neighbors without scanning the entire dataset.

For scalability to billion-scale datasets, modern graph-based ANNS systems typically store their indices on disk [6, 22–24, 43, 50]. They all adopt a coupled layout, where each vector and its corresponding neighbor list are stored contiguously within the same disk page (Figure 3c).

**Product Quantization.** To accelerate distance computations in high-dimensional spaces, many ANNS systems employ product quantization (PQ) [9, 13, 20, 21, 23, 25, 34, 35, 46]. And recent studies also extend it to dynamic scenarios [9, 23, 43, 55]. These PQ codes encode each high-dimensional

#### **Algorithm 1:** Best-first Greedy Search [12]

```
Input: Graph G(V, E), query vector V_q, entry node V_e, result size k, candidate queue size l \geq k

Output: k approximate nearest neighbors to V_q

1 C \leftarrow V_e; // ANN candidate queue

2 Q \leftarrow \emptyset; // visited set

3 while C \setminus Q \neq \emptyset do

4 p^* \leftarrow \arg\min_{V_i \in C \setminus Q} \operatorname{dist\_function}(V_q, V_i);

5 \operatorname{Load} N_{\operatorname{out}}(p^*) from disk;

6 C \leftarrow C \cup N_{\operatorname{out}}(p^*);

7 Q \leftarrow Q \cup \{p^*\};

8 if |C| > l then

9 C \leftarrow \operatorname{Top-} l closest nodes in C to V_q;
```

vector into a compact low-dimensional representation, thereby reducing computational cost. However, since quantization is a form of lossy compression, the inherent information loss means that query accuracy cannot be guaranteed, introducing a probability of retrieval error.

#### 3 Motivation

In this section, we first analyze existing graph-based ANNS systems that couple the topology with vectors and point out their limitations in index updates. We then investigate the root causes of query performance degradation in the decoupled design and propose a naive solution to mitigate it.

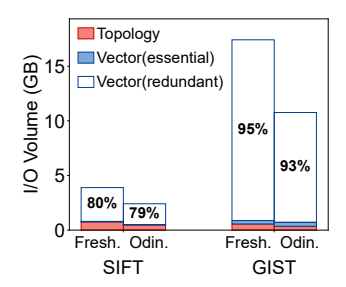
## 3.1 Limitations of Updates in Coupled Index Storage

As discussed in the introduction, the coupled architecture is unfriendly to updates. In this subsection, we will provide a detailed analysis and motivate the purpose of the decoupled storage architecture.

<u>I/O Breakdown and Analysis</u>. To identify the source of the I/O bottleneck (as shown in Figure 1a), we analyze the I/O composition of two representative systems (FreshDiskANN [43] and OdinANN [5, 23]) during index updates. Figure 4 presents the breakdown of I/O volume for topology and vector reads. While vector I/O dominates the total volume, we found that a large fraction is redundant, with many invalid vector reads.

As shown in Figure 4, our analysis reveals that this redundancy constitutes more than 79% of all I/O. This massive inefficiency stems from the tightly coupled storage architecture common in existing graph-based ANNS systems, where vectors are stored within topology on disk. This coupled design forces the system to load them together during topology-only operations, such as graph traversal. Given that vector data is significantly larger than topology data (e.g., on the GIST dataset with a threshold of 32 neighbors, vector data accounts

<sup>&</sup>lt;sup>1</sup>Different graph-based index construction methods adopt different distance-based rules for neighbor pruning or filtering. This work is suitable for all the rules.



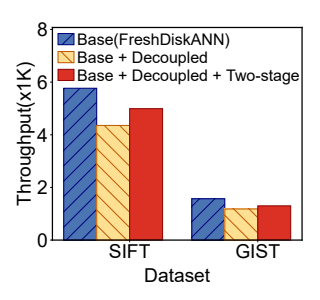


Figure 4: I/O volume breakdown during index update.

Figure 5: Improvement of two-stage query.

for 97% of the total index space), a substantial amount of I/O bandwidth is used to read the invalid vector data. Based on this observation, a direct approach to resolve this inefficiency is to decouple the storage of topology and vectors, thereby ensuring that topology-only operations do not incur accessing redundant vector data.

**Summary.** The significant redundant I/O overhead caused by the coupled storage architecture during updates motivates us to decouple the topology from the graph-based index, enabling index updates to be performed efficiently.

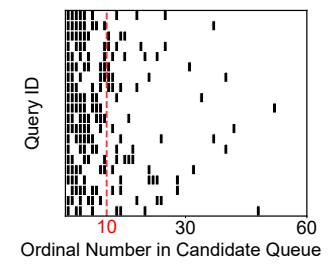
## 3.2 Limitations of Query in Decoupled Index Storage

Although the decoupled storage architecture can improve index update performance, we observe that this design leads to a degradation in query performance, as shown in Figure 1b in the introduction. This subsection reveals the reasons for this degradation and provides a naive solution to this problem.

During query processing, existing systems typically use in-memory PQ-compressed vectors for distance comparisons in the best-first greedy search (line 4 in Algorithm 1), as PQ is computationally much more efficient. However, relying solely on compressed PQ for distance comparison yields limited accuracy. To enhance precision, state-of-the-art methods employ a hybrid strategy. At each step of the search, they perform an exact distance calculation on the most promising candidate (i.e.,  $p^*$  in Algorithm 1, the nearest neighbor that has not been visited so far). These precise distances are then used to maintain an accurately ranked candidate queue. This approach ensures retrieval precision while avoiding the retrieval and computation for all nodes ever seen, thus reducing the computation and I/O overhead.

However, under a decoupled storage architecture, topology and vector data are stored separately. This leads to two random I/O per step during best-first greedy search, doubling both the number and total volume of I/O operations, thereby significantly degrading query performance.

A simple yet effective solution is to separate the exact distance computations from the greedy index search, which we refer to as the *two-stage query*. In the first stage (greedy



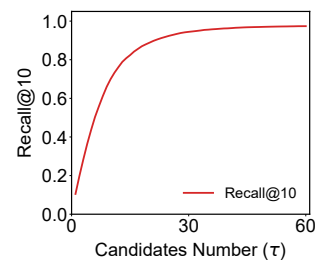


Figure 6: The distribution of true NNs in the candidate queue (k = 10).

Figure 7: Recall improves as the candidates number  $(\tau)$  increases.

search), a best-first greedy search using only PQ-based distances gathers a queue of approximate candidates. In the second stage (rerank), we select top- $\tau$  candidates from the candidate queue, and fetch their vectors from disk for exact distance computation and final reranking, where  $\tau > k$ . By merging multiple scattered reads during the search process into a single batch read, this method reduces random disk access overhead. Additionally, it fully leverages the parallelism of modern SSDs and reduces overall I/O latency. As illustrated in Figure 5, this approach (red bar) yields performance gains of 10% and 14% over the purely decoupled baseline (yellow bar) on the SIFT and GIST datasets. However, it is still lagging behind the original coupled system (blue bar) by 17% and 13%, respectively.

This gap is because of the approximate nature of PQ: with a candidate queue (length l) produced by graph traverse, PQ errors may misorder vectors so that some true NNs (i.e., the actual top-k nearest neighbors) do not appear in the front-k positions, as shown in Figure 6. To ensure accuracy, therefore, instead of selecting the top-k candidates from the queue, we select the top- $\tau$  candidates ( $\tau > k$ ) to obtain the final result. A larger  $\tau$  value yields higher recall, as more candidates are considered. As illustrated in Figure 7, increasing  $\tau$  leads to more accurate query results. However, selecting more candidates from the queue requires reading more vectors from disk and performing more distance computations, thereby increasing both I/O and computational overhead.

In addition, in the first stage, disk page—based reads cause redundant topology data to be fetched, i.e., read amplification. This results in increased I/O overhead in the first stage.

**Summary.** The decoupled architecture increases I/O overhead of ANNS, resulting in reduced query efficiency. Although the two-stage query strategy mitigates this issue, it still incurs substantial I/O overhead due to the larger number of selected candidates and read amplification, particularly when high query precision is required. These limitations motivate us to design a more ingenious query method and data placement strategy that both reduce the number of candidates for exact distance computation and more effectively exploit the data fetched through read amplification during greedy searches.

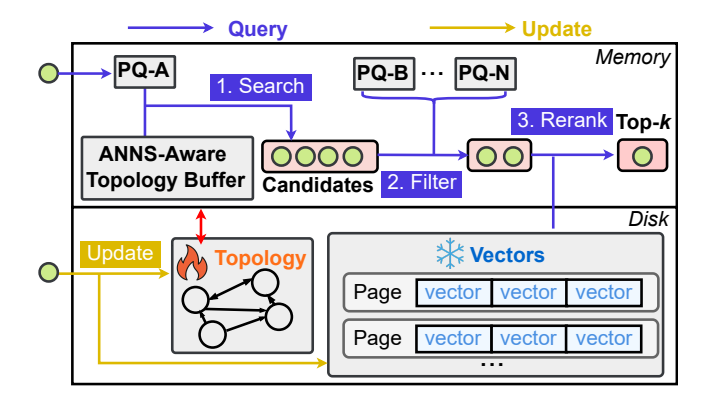


Figure 8: Workflow of the DGAI.

## 4 DGAI Design

Based on the above motivation and observation, we propose a new on-disk graph-based indexing ANNS system, DGAI. In DGAI, we adopt a decoupled storage architecture to enhance update efficiency, and we further design a query engine that is tightly tailored for the decoupled architecture. To begin with, we introduce DGAI's workflow in the query and update process (Section 4.1). We then introduce a three-stage query based on multi-PQs (Section 4.2), which filters out vast redundant overhead and effectively resolves the additional I/O issue during query brought by the decoupled design. Finally, we propose an incremental page-level reordering strategy based on vector similarity (Section 4.3), which places similar nodes on the same page. By coordinating with the caching strategy, this approach effectively leverages fetched redundant data and mitigates the read amplification problem.

#### 4.1 Workflow

We present the workflow of DGAI from two aspects, query and update processing, as illustrated in Figure 8.

<u>Query.</u> The query process, as shown in the upper part of Figure 8 and highlighted in blue, adopts a three-stage query strategy. DGAI first employs PQ-A to perform a greedy search on the graph topology, generating an approximate candidate queue. Then, other PQs refine this queue by filtering out a large number of non-essential candidates, which substantially reduces the number of vectors that need to be accessed in the subsequent step, thereby reducing overall I/O overhead. Finally, the system retrieves the vectors of the remaining candidates, computes their exact distances to the query vector, and returns the top-k nearest neighbors.

<u>Update</u>. The update process is illustrated by the yellow arrows in the lower part of Figure 8. Thanks to the decoupled architecture of topology and vectors, updates in DGAI are divided into two independent procedures: topology updates and vector updates. This separation avoids loading irrelevant data during each procedure, thereby reducing I/O overhead and improving

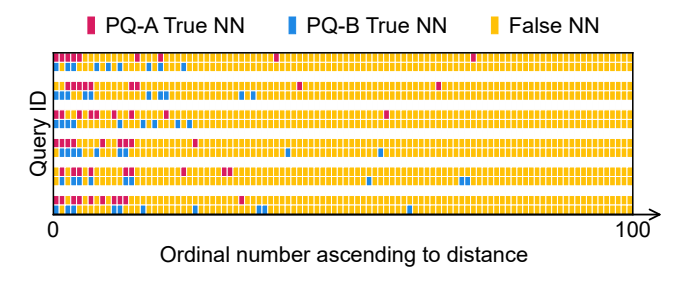


Figure 9: The distribution of true NNs in candidate queues with two PQs (called PQ-A and PQ-B).

update performance. For topology updates, the flexibility of our decoupled design allows it to incorporate diverse graph maintenance strategies [6,31,43] to preserve high index quality. For vector updates, DGAI either writes the new vector into the page or marks the obsolete vector as deleted. To better leverage the decoupled storage architecture, we propose an incremental page-level similarity-aware reordering method for the topology, which enhances data locality and improves cache utilization during update and query processes.

## 4.2 Three-stage Query Based on Multiple PQs

In this subsection, we first analyze the redundancy overhead in queries, and then present a novel three-stage query strategy.

## 4.2.1 Redundancy in ANN Candidate Queue

As discussed in Section 3.2, a simple two-stage query strategy can mitigate the impact of a decoupled storage architecture. However, to achieve higher query accuracy, more candidates must be selected from the candidate queue, requiring vector retrieval from disk and subsequent distance calculations, which leads to substantial I/O and computational overhead. As shown in Figure 7, the recall gain gradually diminishes as  $\tau$  (the number of selected candidates) grows, because enlarging  $\tau$  recovers only a small fraction of true nearest neighbors, i.e., those included in the final top-k results, while introducing a large number of false nearest neighbors, i.e., those excluded from the final top-k results.

To better understand this redundancy, we examined the distribution of true NNs within the candidate queue. Our experiment (10,000 queries on SIFT [10] with l=100) reveals a clear skew: some of the true nearest neighbors for about 1% of queries are incorrectly ranked within the bottom 73% of the candidate queue due to PQ errors. This skewed distribution motivates us to introduce more PQs, enabling them to mutually compensate for errors. As shown in Figure 9, we print the distribution of true NNs in the candidate queue of different queries with two independent PQs. It is shown that some nearest neighbors are misranked toward the end of the candidate queue due to approximation errors in PQ-A, but the ranking obtained from PQ-B can compensate for these errors.

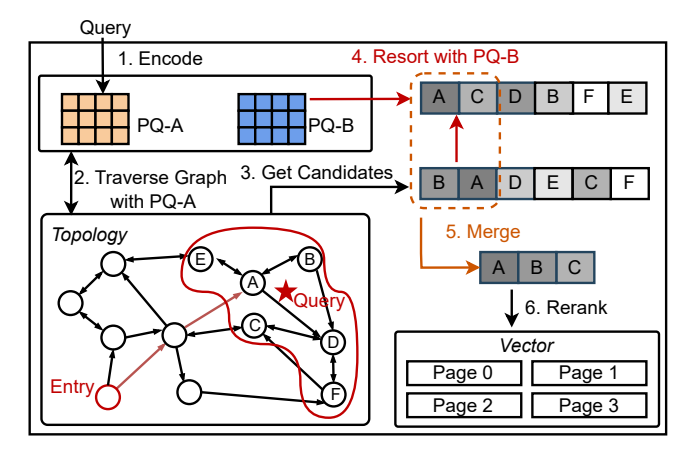


Figure 10: Illustration of three-stage query refinement with multi-PQs filtering (two PQs are shown here for demonstration). The darker shades of grey represent candidates that are closer to the query vector in true distance.

Conversely, errors in PQ-B can be offset by PQ-A. In this way, we can achieve better query results even with a smaller  $\tau$  value. According to the following analysis, the probability that both PQ-A and PQ-B simultaneously misrank the true nearest neighbors toward the end of their candidate queues is very low.

Analysis. The effectiveness of the refined strategy can be explained with a simple probabilistic analysis. Let  $E_i$  denote the event that, in the i-th candidate queue resorted by the i-th PQ, one or more true nearest neighbors are excluded from the top- $\tau$ . We denote the probability of this event as  $P(E_i) = p$ . For c independent PQs, the joint failure probability, i.e., the probability that the true NN(s) are excluded from all resorted queues, is  $P(\bigcap_{i=1}^c E_i) = p^c$ . This exponential decay implies that the probability decreases rapidly as c increases. In other words, by increasing the number of PQs, the system can employ a smaller  $\tau$  while still achieving a comparable recall.

#### 4.2.2 Three-Stage Strategy Design

The above observation motivates a new query strategy that selectively retains only critical candidates from the queue. In detail, DGAI introduces a refinement based on multi-PQs, as illustrated in Figure 10. Specifically, the query consists of three stages: (1) **Greedy search.** The query process starts with a rapid best-first greedy search only using PQ-A to generate an initial ANN candidate queue (Steps 1–3). (2) **Filter.** Then this queue is resorted using PQ-B to yield another independent ordering and take the union of the top-τ candidates from each queue to form a refined candidate queue (Step 4-5). For example, as illustrated in the figure, taking the union of the top-2 candidates from PQ-A and PQ-B produces a refined queue with only 3 candidates, which is sufficient to cover the top-3 nearest neighbors. In contrast, using PQ-A or PQ-B alone

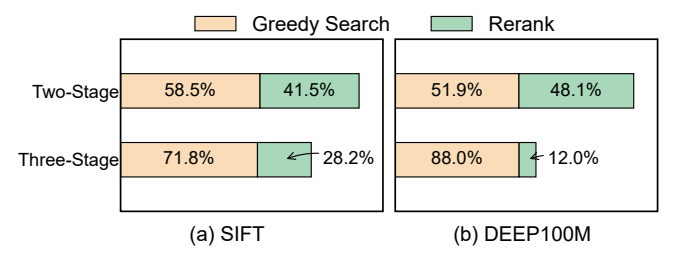


Figure 11: I/O volume breakdown during query execution, comparing the two-stage and our three-stage query on the decoupled architecture.

would require 5 and 4 candidates, respectively. (3) **Rerank.** Finally, the vectors of nodes in the refined candidate queue are retrieved from disk storage for exact distance computation and final reranking (Step 6). This selective refinement strategy reranks only a subset of the most promising candidates, significantly reducing I/O and computational cost.

The remaining problem is how to set the parameter  $\tau$  to achieve a specified recall value. We introduce a warm-up mechanism to estimate  $\tau$ . Specifically, a small sample of queries (e.g., 100) is executed to get a sample set of candidate queues, and then set  $\tau$  to the minimum threshold T that R%(i.e., traget recall) candidate queues hold all true NNs before T on this sample. This ensures that  $\tau$  is large enough to cover nearly all true results while avoiding unnecessary overhead. To further enhance accuracy, we incorporate a dynamic adjustment strategy by defining  $\tau = \min(T \cdot (1 + \log_{10}(l/T)), l)$ , which modestly increases the  $\tau$  when the candidate queue length l is large.

## 4.3 Similarity-Aware Incremental Reordering

While the three-stage query based on multiple PQs significantly reduces I/O requests in the third re-ranking stage, we found that the I/O overhead in the first stage, i.e., greedy search, became the bottleneck. As shown in Figure 11, with the same query recall value (0.98), the proportion of I/O volume in the first stage (greedy search) increases from 51 and 58% to 71 and 88% on the SIFT and DEEP100M datasets, respectively.

Next, we analyze the underlying causes of the high I/O overhead in greedy search and then propose the corresponding solution.

#### 4.3.1 Read Amplification and Topology Layout

The high I/O volume in greedy search primarily stems from read amplification and poor topology locality layout.

**Read Amplification**. In the coupled storage architecture, each page can store only a small number of nodes, especially for high-dimensional datasets (e.g., one node per page for GIST). This ensures that each read incurs minimal invalid data, since both topology and vector are valid, thereby reducing redundant I/O. In the decoupled architecture, reading a single node

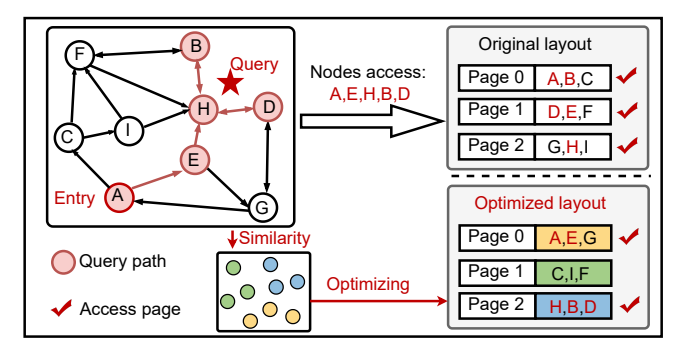


Figure 12: The effect of a better layout.

inevitably brings in a large amount of invalid data, as each page stores a substantial portion of topology information. This results in significant read amplification. For instance, to retrieve the topology of a node with 32 neighbors, which consists of the actual neighbor count and a fixed-length array of 32 neighbor IDs (stored as 32-bit integers, requiring  $33 \times 4$  bytes=132 bytes), the entire 4 KB page (4096 bytes) must be read. Consequently, the read amplification ratio is  $4096/132 \approx 31$ .

One way to mitigate read amplification is to fully exploit the data retrieved during each read. This can be achieved either by computing on all the fetched data [47] or by caching it for subsequent use [59]. However, if the topology layout exhibits poor locality, these approaches often result in wasted computations or a low cache hit rate, thereby increasing computational and memory overhead.

Topology Layout. The best-first greedy search naturally is divided into two phases: approach and converge [22]. In the approach phase, the search rapidly moves toward the query vector. The converge phase, which dominates the overall search time, involves gradual expansion within a small region of the topology to obtain the top-k nearest nodes. This results in frequent access to similar nodes. If the layout of the topology data has strong locality, i.e., similar nodes are co-located on the same page, then a caching strategy can be employed to retain the loaded page for reuse. As illustrated in Figure 12, the original layout requires loading all three pages along the query path. By optimizing the layout based on vector similarity, the number of pages to be loaded is reduced to two, thereby decreasing the overall I/O overhead. This reduces redundant I/O operations and increases cache efficiency by improving the hit rate.

However, we observe that the data often exhibits poor locality. To quantify this, we measure the reuse times of each page during the greedy search. A higher rate signifies strong data locality, meaning more similar nodes are stored in the same page. Our analysis reveals a significant inefficiency. For both benchmark datasets SIFT and GIST, only about 2% of pages are reused more than 2 times. This confirms their poor data locality, where the nodes accessed during a query almost always trigger a new page fetch and random I/O operation

#### Algorithm 2: Incremental Similarity-Aware Reorder

```
Input: New vector v
    Output: Target page of v
 1 N \leftarrow GreedySearch(v); // Sorted in ascending order
      of distance to v
2 \mathcal{P} \leftarrow \{ \text{GetPage}(u) \mid u \in N \};
3 foreach p \in \mathcal{P} do
          if p.size() < MaxCapacity then
 5
               Insert v into page p;
               return p ;
7 p_{old} \leftarrow \text{Getpage}(N[0]);
 \mathbf{8} \ S \leftarrow \texttt{GetNodes}(p_{old});
9 ClearPage(p_{old});
10 p_{new} \leftarrow \text{NewPage}();
11 foreach u \in S do
          if u \notin p_{old} \cup p_{new} then
12
               p_{\text{target}} \leftarrow \arg\min_{p' \in \{p_{old}, p_{new}\}} p'.size();
13
               Insert u into p_{target};
14
15
          else
           p_{\text{target}} \leftarrow \text{GetPage}(u);
16
          foreach w \in Neighbor(u) do
17
               if w \in S \land w \notin p_{old} \cup p_{new} \land p_{target}.size() < |S|/2
18
                     Insert w into p_{target};
20 p^* \leftarrow \text{GetPage}(N[0]);
21 Insert v into p^*;
22 return p^*;
```

instead of reusing a fetched page.

Although several methods [47, 59] have been proposed to improve locality by reordering the topology and thereby mitigating read amplification, these methods are static. When the data changes, the topology must be reordered repeatedly, which introduces significant reordering latency and limits their applicability to dynamic datasets.

#### 4.3.2 Vector Similarity-Aware Graph Topology

To overcome the limitation, DGAI proposes a heuristic incremental reordering algorithm that exploits similarity relationships between newly inserted nodes and their neighbors to optimize the layout of the topology with a better locality. We perform reordering at the page-level rather than at the partition-level because page-level reordering is much lighter and is more friendly to dynamic workloads. Besides, it aligns with the minimum access unit of SSDs, so that each I/O operation can fully benefit from reordering.

Specifically, as shown in Algorithm 2, our incremental reorder mechanism consists of three key steps: (1) Candidate Pages Selection (line 1-2): To insert a new node, we first perform a greedy search to locate the pages containing the nearest existing nodes (top-3 in our evaluation), ensuring that candidate pages are selected based on vector similarity. This step introduces no additional overhead, as the search operation is an integral part of the standard insertion process. (2) Page Insertion Attempt (line 3-6): The system iterates through the candidate pages in ascending order of distance between the new vector and nodes retrieved in step 1. If an available slot is found, the new node is directly inserted. (3) Page Splitting (line 7-21): If all candidate pages are full, the system selects the page containing the nearest node and performs a split operation. Half of the nodes in this page are repartitioned into a new page according to the similarity relation between all nodes in the page. Finally, the new node is inserted into the page where the nearest node resides.

### 5 Implementation and Discussion

**Implementation.** We implement the designs presented in the previous sections in a dynamic ANNS system named DGAI. Furthermore, DGAI integrates another three optimization techniques to enhance both update efficiency and query performance, which we describe in this subsection.

Cache-Aware Computation. We optimize the existing PQbased distance computation in FreshDiskANN and OdinANN with a cache-aware design. Our key design is to transform the memory access pattern by reordering the computation flow. Conventional implementations typically adopt a vectormajor traversal, where distances for each vector are computed across all PQ subspaces. This flow incurs poor cache locality, as codebooks from different subspaces are repeatedly loaded and evicted from the CPU cache. In contrast, our approach employs a subspace-major traversal: distances contributed by one PQ subspace are computed for all vectors before moving to the next subspace. This flow allows the codebook entries of each subspace to remain resident in the CPU cache, substantially reducing memory bandwidth pressure and improving cache reuse. Importantly, this optimization does not alter the computation results, but significantly accelerates distance evaluation.

Query-Level buffer. To further exploit the locality improvements introduced by our reorder mechanism, DGAI introduces a buffer co-designed with the ANNS process to replace the static caching mechanism in the existing systems [23, 43]. Instead of caching both vectors and topology, we cache only graph topology information, which allows more nodes to fit into the same memory size. Building on this, we develop two key components: First, since nodes along a query path are highly correlated while different queries usually traverse disjoint regions, we manage the buffer at the query level. When a query context terminates, all its associated cached pages are evicted, preventing unnecessary memory waste. Second, because all queries start from a fixed entry node, we reserve a small static partition of the buffer for nodes near the entry

Table 1: Benchmark datasets.

Dataset	Dimension	#Vector	Domain	Type
DEEP	96	1,000,000,000	Image	float
SIFT	128	1,000,000	Image	float
MSONG	420	1,000,000	Audio	float
GIST	960	1,000,000	Image	float

point, improving efficiency at the start of the traverse.

<u>Vector Layout Optimization</u>. After our refinement in the second stage, the final stage of the three-stage query process yields a candidate queue where nodes typically share a high similarity in vector space. To capitalize on this property, we apply our incremental reordering method not only to the graph topology but also to the layout of the vectors. By clustering these similar vectors together, this strategy reduces the I/O numbers during the final reranking step to load these vectors. This optimization is particularly effective for low-dimensional datasets, since more nodes can be stored in one page.

**Discussion.** Here we discuss the implications of our decoupled architecture across diverse hardware and algorithms.

Hardware Scalability. Although our current implementation targets SSDs, the decoupled storage design is not bound to any particular hardware and can be readily ported to other platforms. For example, placing the graph topology in persistent memory exploits its byte-addressability, turning slow page-level disk I/O into fast pointer dereferences, thereby accelerating both updates and queries. Likewise, vectors can be offloaded to remote memory via RDMA, which alleviates local storage limitations by utilizing larger memory pools on remote nodes. In summary, DGAI is not a monolithic solution but a flexible architecture that adapts naturally to diverse hardware environments.

Algorithm Scalability. Furthermore, the decoupled storage architecture of DGAI is theoretically applicable to all graph-based indexing methods, such as HNSW. This is because graph-based indices rely heavily on topology as the core structure, which is frequently accessed during both updates and queries. By isolating and optimizing the storage of topology data, DGAI can enhance the efficiency of a wide range of graph-based indices, demonstrating strong algorithm scalability

#### 6 Evaluation

## **6.1** Evaluation Setup.

**Evaluation Platform.** All experiments are conducted on a server equipped with an Intel Xeon Gold 5218R CPU @ 2.10 GHz, 128 GB of DDR4 memory (MICRON 3G2E1, 32 GB × 4), and 7.6 TB of SSD storage (Western Digital SN640 NVMe). The system runs CentOS Linux 7, and all code is compiled using GCC 10.3.0.

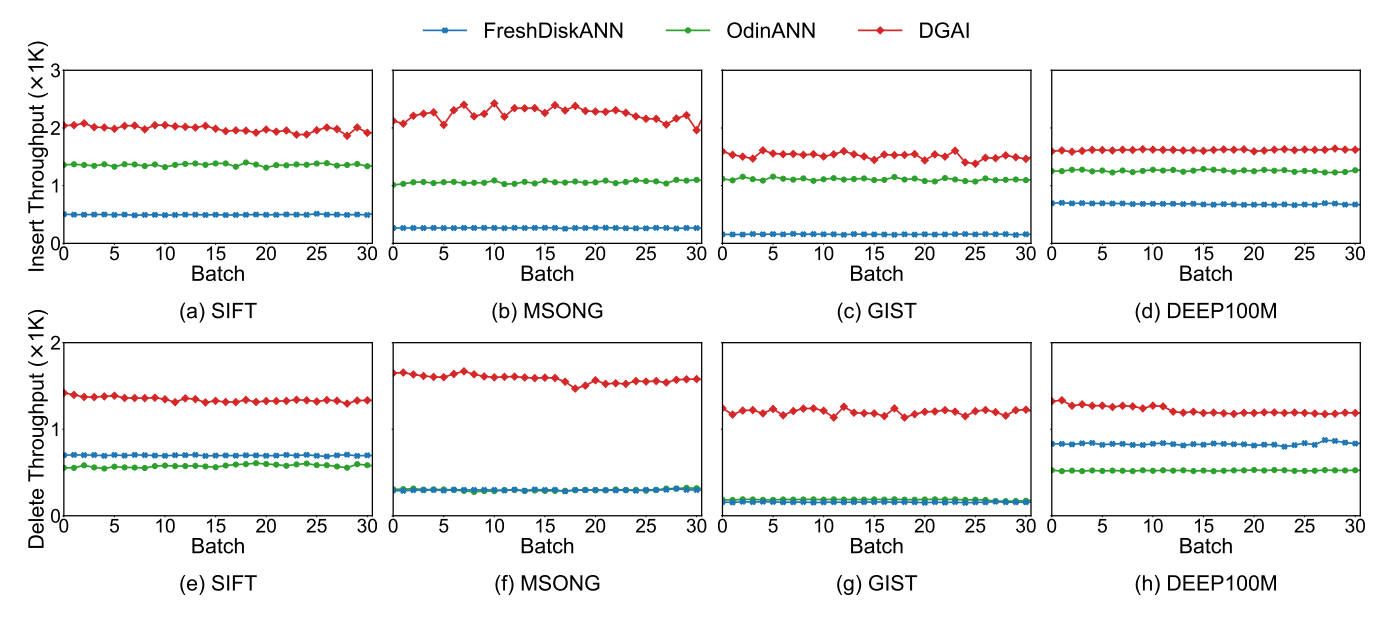


Figure 13: Comparison of update throughput for insert (top) and delete (bottom).

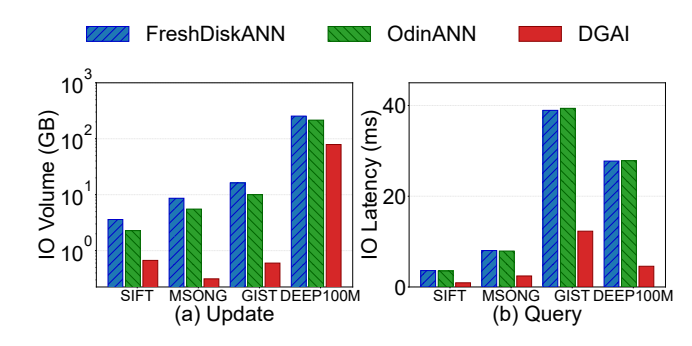


Figure 14: Comparison of I/O in update and query.

**Datasets.** We evaluate our system using four public real-world datasets: DEEP [1], SIFT [10], MSONG [52], and GIST [10], covering a wide range of data dimensionalities (96–960) and scale (1M-1B), with detailed statistics provided in Table 1. Moreover, DEEP1M, DEEP10M, and DEEP100M are subsets of the billion-scale DEEP dataset, which we extract and use for scalability experiments to assess system performance under varying data sizes.

Compared Systems and Parameter Settings. We primarily compare DGAI against two representative dynamic disk-based ANN systems: FreshDiskANN [43] and OdinANN [5, 23]. FreshDiskANN is a pioneering graph-based vector index designed for large-scale datasets on disk, offering low-latency queries and support for incremental updates. OdinANN builds upon FreshDiskANN's core architecture and introduces several key optimizations to improve insertion efficiency by implementing an in-place insertion strategy. These enhancements make OdinANN a more performant and robust solution for insertion-heavy workloads. For a fair comparison against our baselines, FreshDiskANN and OdinANN, we

adopt the same parameter settings to constructed inital index: the maximum number of candidate neighbors during graph construction is set to  $MAX\_C = 160$ , each node maintains up to R = 32 neighbors, and the insertion queue length is limited to  $L\_build = 75$ . In addition, PQ is applied to compress each vector representation into 64 bytes.

#### **6.2** Update Performance

To evaluate the update performance of each system, we first build an initial index using 80% of the dataset vectors. We then conduct 32 rounds of updates for performance measurement, with each round inserting and deleting 1‰ of the total number of indexed vectors. To avoid system fluctuations, the entire procedure is repeated three times, and we report the average results. DGAI uses the same graph structure repair mechanism as the two baselines, ensuring that index quality after updates remains consistent with the baselines. Therefore, in this subsection we focus exclusively on evaluating insertion and update throughput (i.e., the number of operations processed per second).

Insert Performance. Figure 13 (a-d) presents the insertion throughput for all evaluated systems, demonstrating that DGAI consistently delivers superior performance across all benchmarks. Specifically, DGAI achieves a 2.37–10.05× speedup over FreshDiskANN and a 1.29-1.92× speedup over OdinANN. Besides in-place insertion strategy, OdinANN employs an append-only update method that avoids overwriting existing data, enabling fast and sequential insertions with minimal I/O interference. However, this approach causes disk fragmentation and data duplication, leading to index bloat and requiring compaction during deletions, which severely degrades deletion performance.

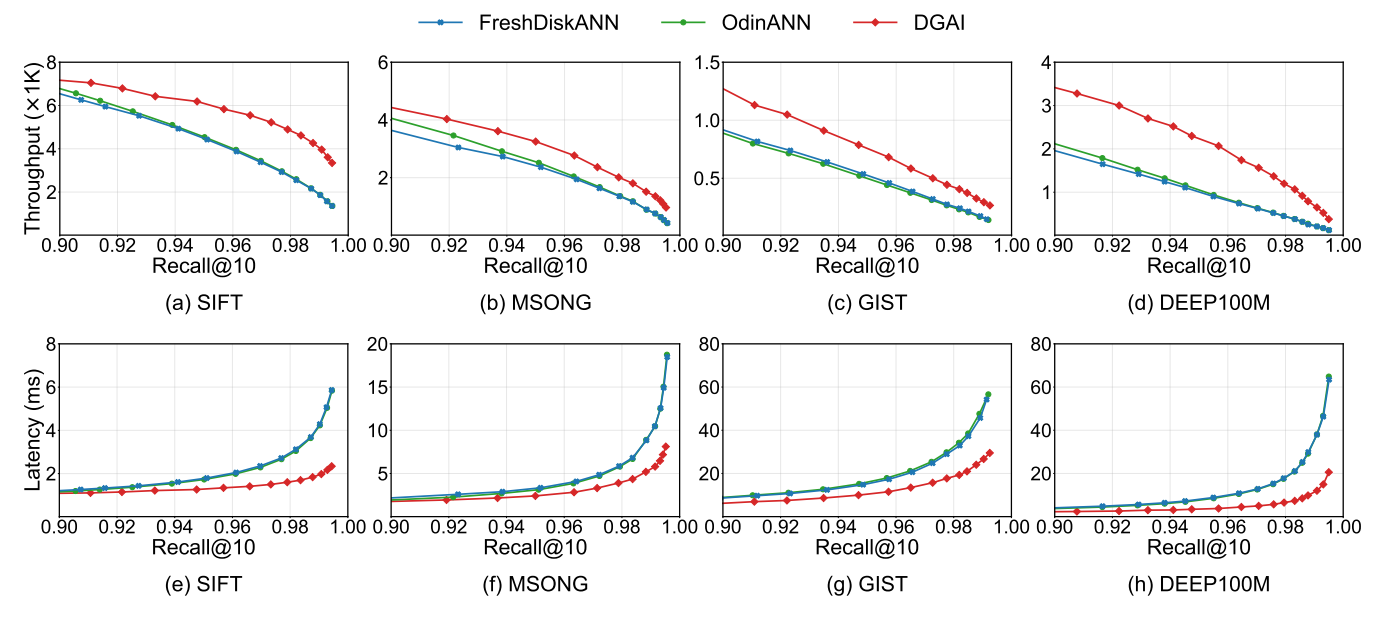


Figure 15: Comparison of query throughput (top) and latency (bottom).

In contrast, DGAI achieves high insertion performance without degrading other workloads, primarily attributed to three key designs: (1) Our three-stage greedy search significantly accelerates the initial stage of neighbor search for the new node (detailed in section 6.3). (2) The incremental vector similarity-aware graph layout co-locates neighbors requiring reverse edge updates within a small number of pages, reducing modified pages and I/O amplification. (3) Our in-place insertion strategy eliminates the merge overhead inherent in batch-based approaches such as FreshDiskANN, ensures stable latency by directly updating the on-disk index.

Delete Performance. Figure 13 (e-f) illustrates the deletion performance, where DGAI consistently and substantially outperforms both FreshDiskANN and OdinANN across all datasets. Specifically, DGAI achieves a 1.47-6.89× speedup over FreshDiskANN and a 2.34-6.12× speedup over OdinANN. As introduced earlier, OdinANN's append-based insertion strategy defers compaction to deletion time, which severely degrades deletion performance, particularly on largescale datasets such as DEEP100M, making it even slower than FreshDiskANN. In contrast, DGAI achieves superior deletion efficiency through two key designs: (1) The decoupled storage architecture avoids loading vectors during topology modifications, reducing I/O cost. (2) The similarity-aware data layout localizes nodes that need to be repaired to maintain graph quantity within the same pages, minimizing random I/O during deletions. Together, these optimizations enable DGAI to consistently outperform both baselines.

To further understand the impact of our optimizations on insertion and deletion, we measure the total I/O volume over the entire update workflow. As shown in Figure 14 (a), DGAI reduces total I/O by 68.98-95.80% compared to FreshDiskANN and by 63.38-93.21% compared to OdinANN. This substan-

tial I/O reduction stems from our decoupled storage architecture and two key designs: avoiding merge overhead (vs. FreshDiskANN) and eliminating compaction costs (vs. OdinANN), while minimizing random I/O through similarity-aware reorder. These highlight the root cause of DGAI 's superior update performance: the substantial alleviation of I/O, which directly leads to higher throughput.

#### **6.3** Query Performance

Figure 15 compares the query performance of all evaluated systems, showing that DGAI consistently achieves superior retrieval efficiency even under an update-friendly storage architecture. Specifically, at 98% recall, DGAI delivers  $1.48-2.66\times$  higher throughput than FreshDiskANN, with query latencies at only 36.61-66.59% of its levels. Compared to OdinANN, DGAI achieves  $1.47-2.63\times$  higher throughput while maintaining just 37.18-67.25% of its latency.

To understand the source of these gains, we analyze I/O behavior during query. Greedy graph search typically follows a synchronous pattern: each expansion step requires loading the neighbors of the current node, computing distances, and selecting the next candidate before proceeding to the next. This sequential dependency leaves disk bandwidth underutilized. In contrast, our three-stage query decouples this process into a fast search stage, a filter stage, and a batched asynchronous vector I/O stage. In the first stage, we leverage the similarity-aware graph layout and an ANNS co-designed buffer to access topology, reducing the I/O counts and volume to minimize the sequential part. In the second stage, multi-PQs filter out redundant nodes from the ANN candidate queue. Finally, the selected vectors are fetched in a single batched asynchronous I/O, better utilizing SSD parallelism.

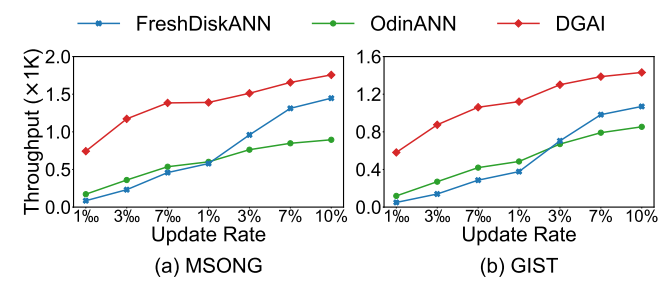


Figure 16: Varying batch size of updates.

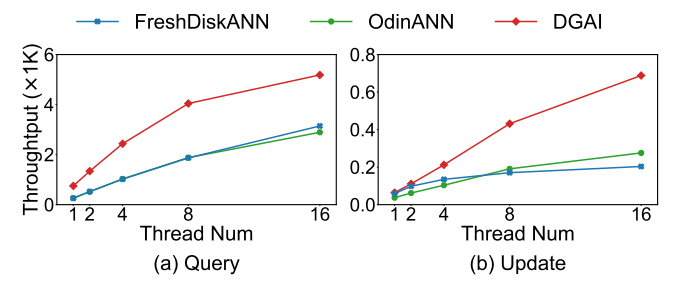


Figure 17: Varying number of threads.

Since sequential dependencies force multiple I/O requests, the I/O volume cannot faithfully reflect the actual query cost. Therefore, we compare I/O latency during query processing, as illustrated in Figure 14 (b). DGAI reduces total query I/O latency by 65.76–82.23% compared to FreshDiskANN and by 64.63–81.67% against OdinANN. These findings elucidate the root cause of the query improvements brought by DGAI.

### 6.4 Sensitivity to Batch Size During Updates

We further evaluate the impact of batch size on update performance by measuring the update throughput on the MSONG and GIST with varying batch sizes (from 1% to 10%), as shown in Figure 16. Since query performance is independent of batch size, update throughput serves as the primary metric.

Compared to FreshDiskANN, DGAI achieves a  $1.67-4.14 \times$  improvement in update throughput, and  $1.95-2.27 \times$  over OdinANN. Despite adopting an in-place insertion mode, DGAI consistently outperforms FreshDiskANN's batch insertion. The advantage is especially pronounced at smaller batch sizes. For example, on the GIST dataset, DGAI achieves a  $1.9 \times$  speedup over FreshDiskANN with an 10% batch size, whereas this speedup increases to  $6.2 \times$  when the batch size is reduced to 1%. Notably, even when the batch size exceeds 7% and the throughput trends of FreshDiskANN and DGAI converge, we still maintain a clear absolute advantage. These results confirm that our in-place update strategy delivers sustained advantages across most of batch sizes.

#### 6.5 Sensitivity to Thread Number

To evaluate system performance under concurrency scenarios, we further assess its update and query scalability in a multi-

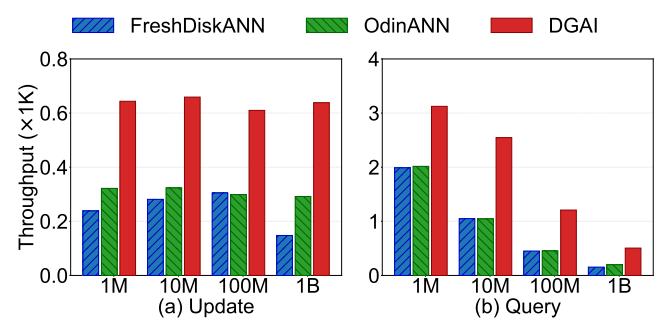


Figure 18: Varying size of benchmark.

threaded environment. We progressively increase the number of concurrent update threads from 1 to 16 and measure the resulting throughput on SIFT. As shown in Figure 17, DGAI outperforms both baseline systems across all thread counts in both query and update workloads.

The scalability gap is particularly evident in update work-loads. In FreshDiskANN and OdinANN, the coupled storage architecture incurs substantial redundant I/O, which causes both systems to saturate SSD bandwidth prematurely. As a result, their throughput plateaus quickly, severely limiting scalability under high concurrency. In contrast, DGAI 's decoupled storage and I/O-efficient update mechanisms avoid this bottleneck, enabling near-linear scaling with thread count.

#### 6.6 Performance on Billion-Scale

We evaluate the performance of DGAI and the two baselines on the DEEP dataset at multiple scales (1M, 10M, 100M, and 1B). As shown in Figure 18, DGAI consistently demonstrates superior performance across all dataset sizes. For update throughput, DGAI consistently outperforms both baselines, achieving average improvements of  $2.30\times$  and  $2.06\times$  over FreshDiskANN and OdinANN, respectively. For query throughput, a downward trend is observed across all systems as the dataset size increases. This is reasonable, as a larger search scope is required to maintain our target 98% recall on larger datasets, leading to increased overhead. Despite this, DGAI maintains a significant lead, outperforming the two baselines by an average of  $2.11\times$  and  $1.97\times$ .

#### 6.7 Performance Gain

To evaluate the contribution of each core design in DGAI to query performance (introduced in Section 4), we incrementally incorporate the proposed components of DGAI. Each configuration is evaluated on two real-world datasets of different scales, SIFT and DEEP100M, with query latency measured at varying recall.

As shown in Figure 19, we first run DGAI without optimizations (i.e., DGAI w/o Optimization) as the baseline. Incorporating the three-stage query with multiple PQs (i.e., DGAI w/ Three-stage) reduces latency by up to 30% on SIFT and 47%

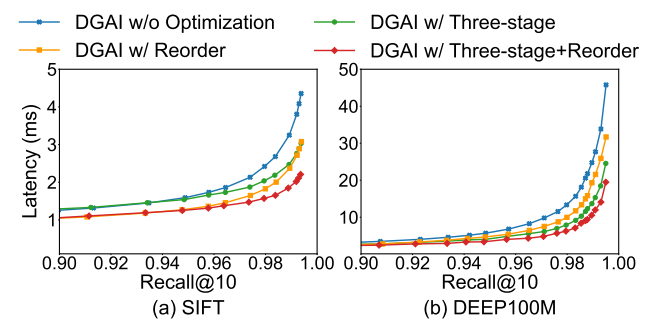


Figure 19: Performance gain.

Table 2: Influence of the number of PQs. c denotes the number of PQs used for filtering;  $\tau$  indicates the number of the candidates; **Filter** refers to the time consumed in the second-stage filtering introduced by additional PQs; **Rerank** refers to the third-stage reranking cost.

	GIST			MSONG		
	c=1	c=2	c=3	c=1	c=2	c=3
Recall@10	98	98	98	98	98	98
τ	548	305	267	137	33	28
Filter (µs)	0	346	533	0	100	151
Rerank (µs)	5528	4192	3925	1142	832	811
Sum (µs)	5528	<u>4538</u>	4458	1142	932	962

on DEEP100M by filtering redundant candidates before the final re-ranking stage. Applying only the incremental similarity—aware reordering and co-designed buffer (i.e., DGAI w/ Reorder) reduces latency by up to 29% and 31% on each dataset by co-locating similar nodes within the same pages, thereby improving buffer efficiency. When both optimizations are combined (i.e., DGAI w/ Three-stage+Reorder), our complete query engine further achieves overall latency reductions of up to 50% on SIFT and 59% on DEEP100M.

## **6.8** Impact of the Number of PQs

We further analyze the impact of varying the number of PQs in the three-stage query on GIST and MSONG. Specifically, we gradually increase the number of candidates  $\tau$  until a recall of 98% is achieved. The final comparison is then made in terms of the summary time.

Table 2 shows that introducing the second PQ allows the same recall to be reached with fewer candidates  $(\tau)$ , thereby reducing redundant computations in the reranking stage and yielding an 18% reduction on both datasets in overall cost compared to using a single PQ. In contrast, adding the third PQ provides only marginal additional benefits, improving efficiency by merely 1.8% on GIST and even degrading 3% on MSONG over the two-PQs, while incurring the extra storage cost of an additional codebook. These results suggest that two PQs strike the best balance between efficiency and overhead, and we adopt this configuration as the default.

#### 7 Related Work

On-disk ANNS Systems. Approximate nearest neighbor search systems on disk are designed to handle massive vector datasets that far exceed the capacity of main memory. In static scenarios, where the dataset is immutable, the main objective is to maximize query performance. This is typically achieved by minimizing costly disk I/O operations while preserving recall, through optimizations in query execution as well as index structures and data layouts [16, 24, 47]. In contrast, dynamic systems face the more complex challenge of efficiently handling frequent updates. This requires a careful balance between sustaining high query performance and minimizing update latency. To address this trade-off, several innovative solutions have emerged. For example, FreshDiskANN [43] is a pioneering graph-based index that introduced support for dynamic operations. Instead of incurring the prohibitive cost of a full index rebuild, it incrementally adjusts the graph in response to updates. This incremental maintenance strategy preserves high index quality and superior query performance, establishing a foundational approach for subsequent dynamic graph-based ANN systems [6, 23, 31, 50].

**Vector Database.** A wide range of database systems has emerged to support efficient management of vector data and to meet increasing demand for vector information requirements [3,6–8,15,29,44,45,48,53,57]. Traditional relational databases such as PostgreSQL [6], and MySQL [4] gradually introduce extensions for vector operations, allowing users to manage vectors within a familiar relational framework. However, because relational engines were not originally designed for high-dimensional vector workloads, their indexing and storage structures are often unable to fully exploit the properties of vectors. As a result, specialized vector databases, such as Milvus [45], are gaining more popularity in the market. By incorporating state-of-the-art ANNS algorithms and hardware optimizations, such systems often deliver higher throughput and better scalability compared to general databases, especially in high-dimensional and large-scale scenarios.

#### 8 Conclusion

We propose DGAI, an on-disk graph-based ANNS system for dynamic workloads. DGAI accelerates index updates by introducing an update-friendly decoupled storage architecture, which separates vector data from the graph index to minimize redundant I/O during updates. Additionally, we propose a novel three-stage query engine, enhanced by an incremental vector similarity-aware layout optimization. Built upon these designs, experiments show that DGAI significantly outperforms two state-of-the-art dynamic graph-based ANNS systems, simultaneously achieving higher update throughput and lower query latency under dynamic workloads.

#### References

- [1] Billion-scale approximate nearest neighbor search challenge: Neurips'21 competition track. https://big-ann-benchmarks.com/, 2021.
- [2] Amazon. https://www.amazon.com, 2025.
- [3] Faiss. https://github.com/facebookresearch/faiss, 2025.
- [4] Mysql. https://dev.mysql.com/, 2025.
- [5] Odinann. https://github.com/thustorage/ PipeANN/blob/main/README-OdinANN.md, 2025.
- [6] pgvector. https://github.com/pgvector/
  pgvector, 2025.
- [7] Pinecone. https://www.pinecone.io, 2025.
- [8] Zilliz. https://zilliz.com/, 2025.
- [9] Cecilia Aguerrebere, Mark Hildebrand, Ishwar Singh Bhati, Theodore Willke, and Mariano Tepper. Locally-adaptive quantization for streaming vector search. *arXiv* preprint arXiv:2402.02044, 2024.
- [10] Laurent Amsaleg and Hervé Jegou. Datasets for approximate nearest neighbor search. http://corpus-texmex.irisa.fr/, 2010.
- [11] Akari Asai, Sewon Min, Zexuan Zhong, and Danqi Chen. Retrieval-based language models and applications. In Proceedings of the 61st Annual Meeting of the Association for Computational Linguistics: Tutorial Abstracts, ACL 2023, Toronto, Canada, July 9-14, 2023, pages 41– 46. Association for Computational Linguistics, 2023.
- [12] Ilias Azizi, Karima Echihabi, and Themis Palpanas. Graph-based vector search: An experimental evaluation of the state-of-the-art. *Proceedings of the ACM on Management of Data*, 3(1):1–31, 2025.
- [13] Artem Babenko and Victor Lempitsky. Additive quantization for extreme vector compression. In *Proceedings* of the IEEE Conference on Computer Vision and Pattern Recognition, pages 931–938, 2014.
- [14] Fu Bang. Gptcache: An open-source semantic cache for llm applications enabling faster answers and cost savings. In *Proceedings of the 3rd Workshop for Natural Language Processing Open Source Software (NLP-OSS 2023)*, pages 212–218, 2023.
- [15] Cheng Chen, Chenzhe Jin, Yunan Zhang, Sasha Podolsky, Chun Wu, Szu-Po Wang, Eric Hanson, Zhou Sun, Robert Walzer, and Jianguo Wang. Singlestore-v: An integrated vector database system in singlestore. *Proc. VLDB Endow.*, 17(12):3772–3785, 2024.

- [16] Qi Chen, Bing Zhao, Haidong Wang, Mingqin Li, Chuanjie Liu, Zengzhong Li, Mao Yang, and Jingdong Wang. SPANN: highly-efficient billion-scale approximate nearest neighborhood search. In Advances in Neural Information Processing Systems 34: Annual Conference on Neural Information Processing Systems 2021, NeurIPS 2021, December 6-14, 2021, virtual, pages 5199–5212, 2021.
- [17] Paul Covington, Jay Adams, and Emre Sargin. Deep neural networks for youtube recommendations. In *Proceedings of the 10th ACM Conference on Recommender Systems, Boston, MA, USA, September 15-19, 2016*, pages 191–198. ACM, 2016.
- [18] Cong Fu, Chao Xiang, Changxu Wang, and Deng Cai. Fast approximate nearest neighbor search with the navigating spreading-out graph. *Proc. VLDB Endow.*, 12(5):461–474, 2019.
- [19] Yunfan Gao, Yun Xiong, Xinyu Gao, Kangxiang Jia, Jinliu Pan, Yuxi Bi, Yi Dai, Jiawei Sun, Qianyu Guo, Meng Wang, and Haofen Wang. Retrieval-augmented generation for large language models: A survey. *CoRR*, abs/2312.10997, 2023.
- [20] Tiezheng Ge, Kaiming He, Qifa Ke, and Jian Sun. Optimized product quantization for approximate nearest neighbor search. In *Proceedings of the IEEE conference on computer vision and pattern recognition*, pages 2946–2953, 2013.
- [21] Yunchao Gong, Svetlana Lazebnik, Albert Gordo, and Florent Perronnin. Iterative quantization: A procrustean approach to learning binary codes for large-scale image retrieval. *IEEE transactions on pattern analysis and machine intelligence*, 35(12):2916–2929, 2012.
- [22] Hao Guo and Youyou Lu. Achieving low-latency graph-based vector search via aligning best-first search algorithm with ssd. In *19th USENIX Symposium on Operating Systems Design and Implementation (OSDI 25)*, pages 171–186, Boston, MA, 2025. USENIX Association.
- [23] Hao Guo and Youyou Lu. Odinann: Direct insert for consistently stable performance in billion-scale graphbased vector search. In 24th USENIX Conference on File and Storage Technologies (FAST 26), Santa Clara, CA, 2026. USENIX Association.
- [24] Suhas Jayaram Subramanya, Fnu Devvrit, Harsha Vardhan Simhadri, Ravishankar Krishnawamy, and Rohan Kadekodi. Diskann: Fast accurate billion-point nearest neighbor search on a single node. *Advances in neural information processing Systems*, 32, 2019.

- [25] Herve Jegou, Matthijs Douze, and Cordelia Schmid. Product quantization for nearest neighbor search. *IEEE transactions on pattern analysis and machine intelligence*, 33(1):117–128, 2010.
- [26] Zhi Jing, Yongye Su, Yikun Han, Bo Yuan, Haiyun Xu, Chunjiang Liu, Kehai Chen, and Min Zhang. When large language models meet vector databases: A survey. *arXiv preprint arXiv:2402.01763*, 2024.
- [27] Patrick S. H. Lewis, Ethan Perez, Aleksandra Piktus, Fabio Petroni, Vladimir Karpukhin, Naman Goyal, Heinrich Küttler, Mike Lewis, Wen-tau Yih, Tim Rocktäschel, Sebastian Riedel, and Douwe Kiela. Retrieval-augmented generation for knowledge-intensive NLP tasks. In Advances in Neural Information Processing Systems 33: Annual Conference on Neural Information Processing Systems 2020, NeurIPS 2020, December 6-12, 2020, virtual, 2020.
- [28] Huayang Li, Yixuan Su, Deng Cai, Yan Wang, and Lemao Liu. A survey on retrieval-augmented text generation. *CoRR*, abs/2202.01110, 2022.
- [29] Jie Li, Haifeng Liu, Chuanghua Gui, Jianyu Chen, Zhenyuan Ni, Ning Wang, and Yuan Chen. The design and implementation of a real time visual search system on JD e-commerce platform. In *Proceedings of the 19th International Middleware Conference, Middleware Industrial Track 2018, Rennes, France, December 10-14, 2018*, pages 9–16. ACM, 2018.
- [30] Nan Li, Bo Kang, and Tijl De Bie. Skillgpt: a restful API service for skill extraction and standardization using a large language model. *CoRR*, abs/2304.11060, 2023.
- [31] Dawei Liu, Bolong Zheng, Ziyang Yue, Fuhao Ruan, Xiaofang Zhou, and Christian S Jensen. Wolverine: Highly efficient monotonic search path repair for graph-based ann index updates.
- [32] Yury Malkov, Alexander Ponomarenko, Andrey Logvinov, and Vladimir Krylov. Approximate nearest neighbor algorithm based on navigable small world graphs. *Inf. Syst.*, 45:61–68, 2014.
- [33] Yury A. Malkov and Dmitry A. Yashunin. Efficient and robust approximate nearest neighbor search using hierarchical navigable small world graphs. *IEEE Trans. Pattern Anal. Mach. Intell.*, 42(4):824–836, 2020.
- [34] Julieta Martinez, Joris Clement, Holger H Hoos, and James J Little. Revisiting additive quantization. In *European Conference on Computer Vision*, pages 137–153. Springer, 2016.

- [35] Julieta Martinez, Shobhit Zakhmi, Holger H Hoos, and James J Little. Lsq++: Lower running time and higher recall in multi-codebook quantization. In *Proceedings* of the European conference on computer vision (ECCV), pages 491–506, 2018.
- [36] Yitong Meng, Xinyan Dai, Xiao Yan, James Cheng, Weiwen Liu, Jun Guo, Benben Liao, and Guangyong Chen. PMD: an optimal transportation-based user distance for recommender systems. In Advances in Information Retrieval 42nd European Conference on IR Research, ECIR 2020, Lisbon, Portugal, April 14-17, 2020, Proceedings, Part II, volume 12036 of Lecture Notes in Computer Science, pages 272–280. Springer, 2020.
- [37] Jason Mohoney, Anil Pacaci, Shihabur Rahman Chowdhury, Ali Mousavi, Ihab F. Ilyas, Umar Farooq Minhas, Jeffrey Pound, and Theodoros Rekatsinas. Highthroughput vector similarity search in knowledge graphs. *Proc. ACM Manag. Data*, 1(2):197:1–197:25, 2023.
- [38] Shumpei Okura, Yukihiro Tagami, Shingo Ono, and Akira Tajima. Embedding-based news recommendation for millions of users. In *Proceedings of the 23rd ACM SIGKDD International Conference on Knowledge Discovery and Data Mining, Halifax, NS, Canada, August 13 17, 2017*, pages 1933–1942. ACM, 2017.
- [39] Sajal Regmi and Chetan Phakami Pun. GPT semantic cache: Reducing LLM costs and latency via semantic embedding caching. *CoRR*, abs/2411.05276, 2024.
- [40] Keshav Santhanam, Omar Khattab, Jon Saad-Falcon, Christopher Potts, and Matei Zaharia. Colbertv2: Effective and efficient retrieval via lightweight late interaction. In Proceedings of the 2022 Conference of the North American Chapter of the Association for Computational Linguistics: Human Language Technologies, NAACL 2022, Seattle, WA, United States, July 10-15, 2022, pages 3715–3734. Association for Computational Linguistics, 2022.
- [41] Badrul Munir Sarwar, George Karypis, Joseph A. Konstan, and John Riedl. Item-based collaborative filtering recommendation algorithms. In *Proceedings of the Tenth International World Wide Web Conference, WWW 10, Hong Kong, China, May 1-5, 2001*, pages 285–295. ACM, 2001.
- [42] Luis Gaspar Schroeder, Shu Liu, Alejandro Cuadron, Mark Zhao, Stephan Krusche, Alfons Kemper, Matei Zaharia, and Joseph E. Gonzalez. Adaptive semantic prompt caching with vectorq. *CoRR*, abs/2502.03771, 2025.
- [43] Aditi Singh, Suhas Jayaram Subramanya, Ravishankar Krishnaswamy, and Harsha Vardhan Simhadri.

- Freshdiskann: A fast and accurate graph-based ANN index for streaming similarity search. *CoRR*, abs/2105.09613, 2021.
- [44] Yongye Su, Yinqi Sun, Minjia Zhang, and Jianguo Wang. Vexless: A serverless vector data management system using cloud functions. *Proc. ACM Manag. Data*, 2(3):187, 2024.
- [45] Jianguo Wang, Xiaomeng Yi, Rentong Guo, Hai Jin, Peng Xu, Shengjun Li, Xiangyu Wang, Xiangzhou Guo, Chengming Li, Xiaohai Xu, Kun Yu, Yuxing Yuan, Yinghao Zou, Jiquan Long, Yudong Cai, Zhenxiang Li, Zhifeng Zhang, Yihua Mo, Jun Gu, Ruiyi Jiang, Yi Wei, and Charles Xie. Milvus: A purpose-built vector data management system. In SIGMOD '21: International Conference on Management of Data, Virtual Event, China, June 20-25, 2021, pages 2614–2627. ACM, 2021.
- [46] Jun Wang, Wei Liu, Sanjiv Kumar, and Shih-Fu Chang. Learning to hash for indexing big data—a survey. *Proceedings of the IEEE*, 104(1):34–57, 2015.
- [47] Mengzhao Wang, Weizhi Xu, Xiaomeng Yi, Songlin Wu, Zhangyang Peng, Xiangyu Ke, Yunjun Gao, Xiaoliang Xu, Rentong Guo, and Charles Xie. Starling: An i/o-efficient disk-resident graph index framework for high-dimensional vector similarity search on data segment. *CoRR*, abs/2401.02116, 2024.
- [48] Chuangxian Wei, Bin Wu, Sheng Wang, Renjie Lou, Chaoqun Zhan, Feifei Li, and Yuanzhe Cai. Analyticdb-v: A hybrid analytical engine towards query fusion for structured and unstructured data. *Proc. VLDB Endow.*, 13(12):3152–3165, 2020.
- [49] Kyle Williams, Lichi Li, Madian Khabsa, Jian Wu, Patrick C. Shih, and C. Lee Giles. A web service for scholarly big data information extraction. In 2014 IEEE International Conference on Web Services, ICWS, 2014, Anchorage, AK, USA, June 27 - July 2, 2014, pages 105– 112. IEEE Computer Society, 2014.
- [50] Haike Xu, Magdalen Dobson Manohar, Philip A. Bernstein, Badrish Chandramouli, Richard Wen, and Harsha Vardhan Simhadri. In-place updates of a graph index for streaming approximate nearest neighbor search. *CoRR*, abs/2502.13826, 2025.
- [51] Yuming Xu, Hengyu Liang, Jin Li, Shuotao Xu, Qi Chen, Qianxi Zhang, Cheng Li, Ziyue Yang, Fan Yang, Yuqing Yang, Peng Cheng, and Mao Yang. Spfresh: Incremental in-place update for billion-scale vector search. In *Pro*ceedings of the 29th Symposium on Operating Systems Principles, SOSP 2023, Koblenz, Germany, October 23-26, 2023, pages 545–561. ACM, 2023.

- [52] Mingyu Yang, Wentao Li, and Wei Wang. Fast high-dimensional approximate nearest neighbor search with efficient index time and space, 2025.
- [53] Wen Yang, Tao Li, Gai Fang, and Hong Wei. PASE: postgresql ultra-high-dimensional approximate nearest neighbor search extension. In *Proceedings of the 2020 International Conference on Management of Data, SIG-MOD Conference 2020, online conference [Portland, OR, USA], June 14-19, 2020*, pages 2241–2253. ACM, 2020.
- [54] Zhi Yao, Zhiqing Tang, Jiong Lou, Ping Shen, and Weijia Jia. VELO: A vector database-assisted cloud-edge collaborative LLM qos optimization framework. In *IEEE International Conference on Web Services, ICWS* 2024, Shenzhen, China, July 7-13, 2024, pages 865–876. IEEE, 2024.
- [55] Song Yu, Shengyuan Lin, and Shufeng Gong. A topology-aware localized update strategy for graph-based ann index. *arXiv preprint arXiv:2503.00402*, 2025.
- [56] Yuanhang Yu, Dong Wen, Ying Zhang, Lu Qin, Wenjie Zhang, and Xuemin Lin. Gpu-accelerated proximity graph approximate nearest neighbor search and construction. In 2022 IEEE 38th International Conference on Data Engineering (ICDE), pages 552–564. IEEE, 2022.
- [57] Qianxi Zhang, Shuotao Xu, Qi Chen, Guoxin Sui, Jiadong Xie, Zhizhen Cai, Yaoqi Chen, Yinxuan He, Yuqing Yang, Fan Yang, Mao Yang, and Lidong Zhou. VBASE: unifying online vector similarity search and relational queries via relaxed monotonicity. In 17th USENIX Symposium on Operating Systems Design and Implementation, OSDI 2023, Boston, MA, USA, July 10-12, 2023, pages 377–395. USENIX Association, 2023.
- [58] Weijie Zhao, Shulong Tan, and Ping Li. Song: Approximate nearest neighbor search on gpu. In 2020 IEEE 36th International Conference on Data Engineering (ICDE), pages 1033–1044. IEEE, 2020.
- [59] Yijie Zhou, Shengyuan Lin, Shufeng Gong, Song Yu, Shuhao Fan, Yanfeng Zhang, and Ge Yu. Govector: An i/o-efficient caching strategy for high-dimensional vector nearest neighbor search. *arXiv* preprint arXiv:2508.15694, 2025.